Korea Polymer Journal, Vol. 8, No. 2, pp 95 – 101 (2000)

Effects of Intercalant on the Dispersibility of Silicate Layers in Clay-dispersed Nanocomposite of Poly(styrene-*co*-acrylonitrile) Copolymer

Moon Bae Ko*, Min Park, Junkyung Kim, Chul Rim Choe

Polymer Hybrid Research Center, Korea Institute of Science and Technology, Seoul 130-650, Korea

Received March 8, 2000

Abstract : Clay/poly(styrene-*co*-acrylonitrile) copolymer (SAN) hybrids have been prepared by simple meltmixing of two components, SAN and organophilic clays with a twin screw extruder. Effects of intercalant on the dispersibility of silicate layers in clay-dispersed nanocomposite were studied by using five different organophilic clays modified with the intercalants of different chemical structures and different fractions of intercalant. The dispersibility of 10-Å-thick silicate layers of clay in the hybrid was investigated by using an X-ray diffractometer and a transmission electron microscope. It was found that if the fraction of intercalant in the organophilic clay becomes too high, SAN is difficult to intercalate into the inter-gallery of silicate layers in the hybrid prepared at 180°C, and thus the hybrid shows poor dispersibility of silicate layers. The flexural modulus of the hybrid increases as the dispersibility of silicate layers in the hybrid increases.

Introduction

Hybrid organic-inorganic composites typically exhibit mechanical properties superior to those of their separate components. To optimize the performance of these materials, it is usually desirable to disperse the inorganic components in the organic matrix on a nanometer length scale. A good method for the preparation of organic-inorganic nanocomposites is that disperses smectite clays and other layered inorganic materials that can be broken down into nanoscale building blocks.[1-13] In general, the clay/polymer composites can be divided into three categories: conventional composites, intercalated nanocomposites, and exfoliated nanocomposites. In a conventional composite, the clay tactoids exist in their original aggregated state with no intercalation of the polymer matrix into the clay. In an intercalated nanocomposite the insertion of polymer into the clay structure occurs in a crystallographically regular fashion, regardless of the clay-to-polymer ratio. An intercalated nanocomposite normally is interlayered by only a few molecular layers of polymer and the properties of the composite typically resemble those of the ceramic host. In contrast, in an exfoliated nanocomposite, the individual 10-Å-thick clay layers are separated in a continuous polymer matrix by average distance that depends on the loading of clay.

Three different methods for preparing clay-dispersed nanocomposites are well known up to now: i) solution drying, ii) monomer intercalation-polymerization, and iii) direct polymer intercalation-compounding methods. Recently, the third method has received an extensive interest because polymers can be inserted directly into the layered material without the aid of solvent. Subsequent shearing in a melt mixer allows the individual clay layer to be dispersed homogeneously in a matrix polymer.

Styrenic polymers, e.g. polystyrene (PS), poly (styrene-*co*-acrylonitrile) copolymer, acrylonitrile-butadiene-styrene resin, and high impact polystyrene, are widely used as the matrix. Thus many researchers have been interested in clay/PS hybrids. Vaia *et al.*[14] reported the intercalation behavior of PS into organophilic clay above the glass transition temperature of PS. Akelah and Moet,[15] also,

* e-mail : mbko@kistmail.kist.re.kr

prepared clay/PS hybrids by polymerization of styrene in the existence of organophilic clay. Researchers at Toyota,[16] recently, reported clay/PS hybrids prepared by melt-blending polystyrene with organophilic clay. They used styrenemethylvinyloxazoline copolymer by including small amount of oxazoline group in order to facilitate the intercalation of PS into the inter-gallery of silicate layers.

In the present work, clay/SAN hybrids have been prepared by simple melt-mixing of two components, i.e., SAN and five different organophilic clays with a twin screw extruder at 180°C. The dispersibility of 10-Å-thick silicate layers in the hybrids was investigated by using a transmission electron microscope and an X-ray diffractometer. Also, the intercalation behavior was studied by monitoring the change of XRD patterns from the hybrids prepared by annealing the mixtures of organophilic clays and SAN powder in zero-shear rate condition at the same temeprature, 180°C.

Experimental

Materials. "Cloisite®" supplied by Southern Clay Products is trade name of organophilic clays with various cation exchange capacities. Also, three kinds of intercalants were used in the study: dimethyl dihydrogenated tallow ammonium (2M2HT), dimethyl hydrogenated-tallow (2-ethylhexyl) ammonium (2MHTL8), and methyl tallow bis-2hydroxyethyl ammonium (MT-2EthOH). The chemical structures of intercalants are depicted in Figure 1, where HT is predominantly an octadecyl chain with smaller amounts of lower homologues (approximate composition: ~65% C18, ~30% C16, ~5% C14). Its inorganic content was calculated by measuring the weights before and after burning its organic parts. Also, the basal spacing

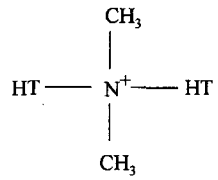

2M2HT

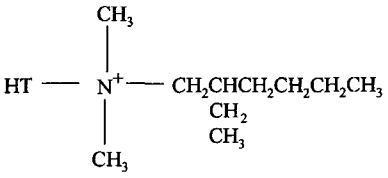

2MHTL8

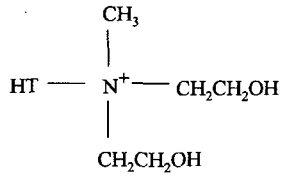

MT-2EthOH

Figure 1. Chemical structures of intercalants used in the study.

of organophilic clay was measured by X-ray diffraction method. The characteristic properties of organophilic clays are summarized in Table I. Poly (styrene-*co*-acrylonitrile) copolymer, of which the acrylonitrile content was 25 wt%, was obtained from Cheil Industries Inc., and it was used after drying in a vacuum oven at 80°C for more than 24 hours.

Preparation of Hybrids. The mixtures of organophilic clays and SAN powder with a narrow particle size distribution, which was collected

Table I. Charateristic Properties of the Organophilic Clays Used in the Study.

Code	Organic Modifier	Modifier Concentration (meq/100g)	Weight Loss on Ignition (%)	*d*-spacing (Å)
C1	2M2HT	140	47	35.6
C2	2M2HT	125	43	32.2
C3	2M2HT	95	38	25.7
C4	2MHTL8	95	34	20.0
C5	MT-2EthOH	95	32	18.2

using a Cu mesh sieve (180 mesh) before dry-blending, were pressed for predetermined annealing times at 180°C, in order to investigate the hybrids prepared without shear force. Also the hybrids were prepared by compounding method. Two powdery components of organophilic clay and SAN were dry-mixed, and then the mixture was melt-blended by using a twin screw extruder (Model TSE-16-TC, Prism) at 180°C and 100 rpm to yield pale-yellow strand of the hybrids. The obtained strands were chopped with a pelletizer, and were extruded again with the twin screw extruder. The inorganic content in the hybrids was fixed at 5 wt% in this study.

Evaluation of the Clay Dispersibility in SAN matrix. The dispersibility of silicates layers in the hybrids was evaluated by using an X-ray diffractometer and a transmission electron microscope (TEM). An X-ray diffractometer (Model MXP18, MacScience) was adopted to monitor the change in *d*-spacing of montmorillonite before and after intercalation. CuK_{α} ($\lambda = 1.54$Å) was used as X-ray source at a generator voltage of 40 kV and current of 100 mA. The scanning rate was 0.2 °/min. The basal spacing of the silicate layers, *d*, was calculated using the Bragg's law, $\lambda = 2d\sin\theta$ from the position of the (001) plane peak in the XRD pattern. TEM (Model CN30, Philips) observations of the hybrids were performed for the injection-molded samples, and were operated at an acceleration voltage of 120 kV. Thin sections of 70 nm were microtomed with a diamond knife and then subjected to TEM observation without staining.

Measuring the Mechanical Properties of Hybrids. The flexural tests were carried out with an Instron Model 4201 at room temperature. The crosshead speed was 1 mm/min. All measurements were performed for five replicates of rectangular specimens which were injection-molded with a Mini-Max molder and the reported value is the mean value of those five measurements.

Results and discussion

Intercalation Capability of SAN. Figure 2(a) shows the XRD patterns of the various organophilic clay powders. The measured basal spacings of clays are tabulated in Table I, which shows that the basal spacing increases as the quantity of organic part in organophilic clays increases. Simple calculation on the gallery heights of organophilic clays with bilayer or trilayer arrangements of alkyl chains in organic modifier may support the explanation: $d_{bilayer} = 9.6 + 2 \times 4.6 = 18.8$ (Å) (corresponding to $2\theta \sim 4.7°$) for bilayer, and $d_{trilayer} = 9.6 + 3 \times 4.6 = 23.4$ (Å) (corresponding to $2\theta \sim 3.8°$) for trilayer. In the calculations, 9.6 and 4.6Å were used as the thickness of silicate layer and that of alkyl chain in monolayer-arrangement, respec-

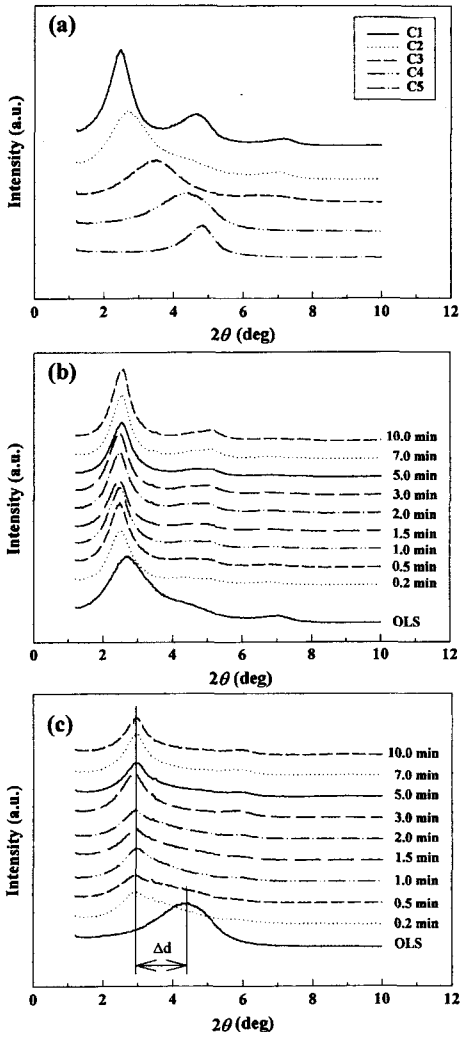

Figure 2. X-ray patterns of (a) the powders of organophilic clays; (b) C2/SAN-hybrids; (c) C4/SAN-hybrids annealed for the times indicated in the figures.

tively.[17-19] So it is well explained that while the structure of alkyl ammonium ion in the inter-gallery of silicate layers is bi-layer in C4- and C5-clays, and that in C3-clay is tri-layer, those in C1- and C2-clays do not show a layered structure, but paraffin-like structures. Figure 2(b) and 2(c) are the temporal series of XRD patterns from the C2/SAN- and C4/SAN-hybrids annealed at 180°C. It can be found that while the positions of (001) peak in the XRD patterns of C2/SAN-hybrid do not shift much, those of C4/SAN-hybrid shift to a lower angle $2\theta = 2.96°$ from $2\theta = 4.42°$ in very short time. This means that SAN molecules can intercalate into inter-gallery of silicate layers upon annealing the mixture of the organophilic clay and SAN. The driving force for the intercalation of SAN molecule might originate from a strong hydrogen-bonding between hydroxyl groups on the surface of silicates and the nitrile group of SAN. It is also noteworthy that the positions of (001) plane peak in XRD patterns of C4/SAN-hybrid do not shift much after 0.2 min, irrespective of annealing time.

Figure 3(a) shows the plots of basal spacing of organophilic clay in the hybrid as a function of annealing time. The basal spacing of organophilic clay decreases as the fraction of organic modifier in the organophilic clay decreases, but that of C5-clay hybrid is larger than that of C4-clay hybrid, and is smaller than that of C3-clay hybrid. The change of basal spacing, Δd, is defined as the difference between (001) peak positions on the XRD patterns of the organophilic clay-powder and annealed hybrid. Δd's for various clay/SAN hybrids are plotted in Figure 3(b), which shows that the change of basal spacing increases as the fraction of organic modifier in the organophilic clay decreases. In case of tri-layer or bi-layer structure of intercalant such as in C3-, C4-, and C5-clays, there are vacant sites through which SAN molecules can easily diffuse into the inter-gallery of silicate layers. It is well known that the intercalants reorient from their initial bi-layer, tri-layer or paraffin-like orientation to a vertical orientation after the intercalation of polymer or low molecular weight molecules. Thus the magnitude of change in basal spacing, Δd, increases as the fraction of organic modifier in the organophilic clay decreases.

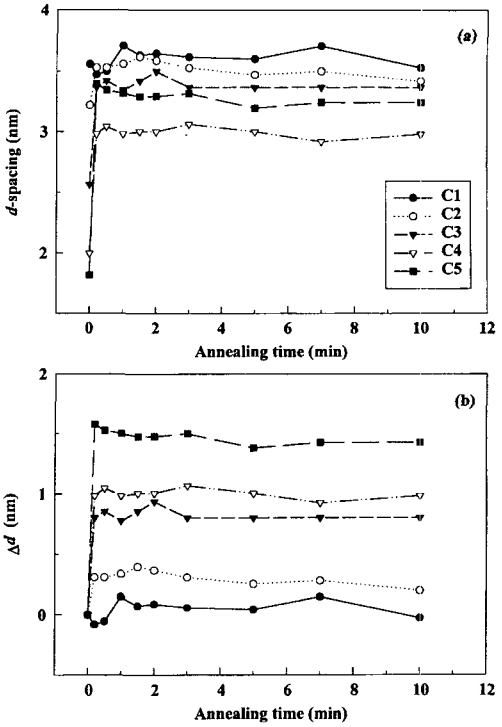

Figure 3. (a) Plots of the basal spacing of clay layers; (b) Plots of the change of basal spacing, Δd as a function of annealing time upon annealing the mixture of the organophilic clays and SAN powder.

Full width at half maximum of the (001) peak can also be used to determine the thickness of intercalated silicate crystallite. Small crystallites give broad Bragg reflections, and a simple way of assessing the crystallite thickness perpendicular to a given set of (001) planes is through the Scherrer equation[20]:

$$\bar{D}_{001} = \frac{K\lambda}{\beta \cos\theta} \quad (1)$$

where K is the Scherrer shape factor which adopts value close to unity, and β is the breadth (in radians, at half the peak value) of the diffraction peak associated with (001) planes. The measured crystallite thicknesses of silicate layers associated with (001) reflection are plotted as a function of annealing time in Figure 4(a). Dividing the crystallite thickness by the d-spacing of organophilic clay, the average number of silicate layers associated with (001) reflection can be calculated. Figure

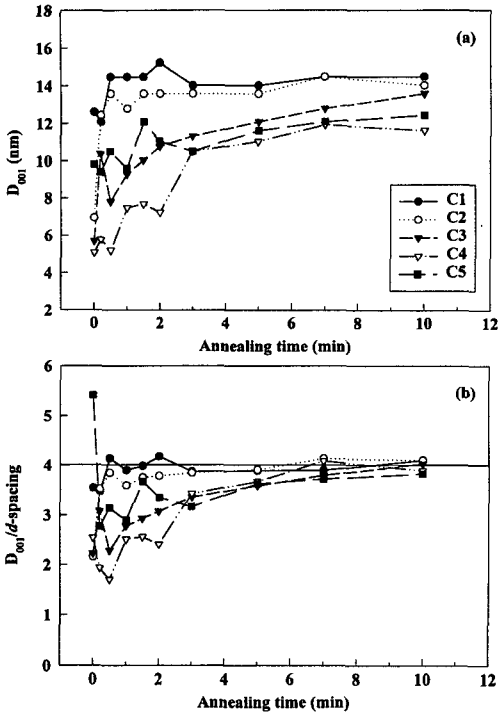

Figure 4. (a) Plots of the crystallite-thickness of silicate layers associated with (001) reflection; (b) Plots of the number of silicate layers separated by the distance of *d*-spacing in a crystallite as a function of annealing time upon annealing the mixture of the organophilic clays and SAN powder.

4(b) shows the change of the average number of silicate layers associated with (001) reflection with annealing time for various clay/SAN hybrids. The numbers in C1- and C2-clay hybrids are not so much changed from the beginning of annealing, but those in C3-, C4-, and C5-clay hybrids increase with increasing the annealing time after 0.2 min. Although the *d*-spacing of organophilic clays increases at the first stage of annealing, the average number of expanded inter-galleries increases gradually with increasing the annealing time. This is due to the fact that the unexpanded inter-galleries of organophilic clay also expand as the further intercalation of SAN molecules into the unexpanded inter-gallery takes place upon annealing the mixture for more time. Even though some fluctuations can be found at the first stage of annealing, it is noteworthy that the average numbers of silicate layers associated with (001) reflection increase and converge to about 4 after 5 minutes, irrespective of the kind of organophilic clays.

Dispersibility of Clay Layers in the Hybrid. The mixtures were melt-mixed twice with a twin-screw extruder at 180°C. In order to confirm the hybrid structures, the dispersibility of silicate layers in the hybrids was observed by using a transmission electron microscope. Figure 5 is the TEM micrographs, which show that nano-scale building blocks are distributed homogeneously in the sample. Any other evidence for truly exfoliated nanocomposite could not be found in the study. However, it can be said that the nano-scale building block becomes smaller as the fraction of intercalant in the organophilic clay becomes lower though a quantitative analysis for the dispersibility

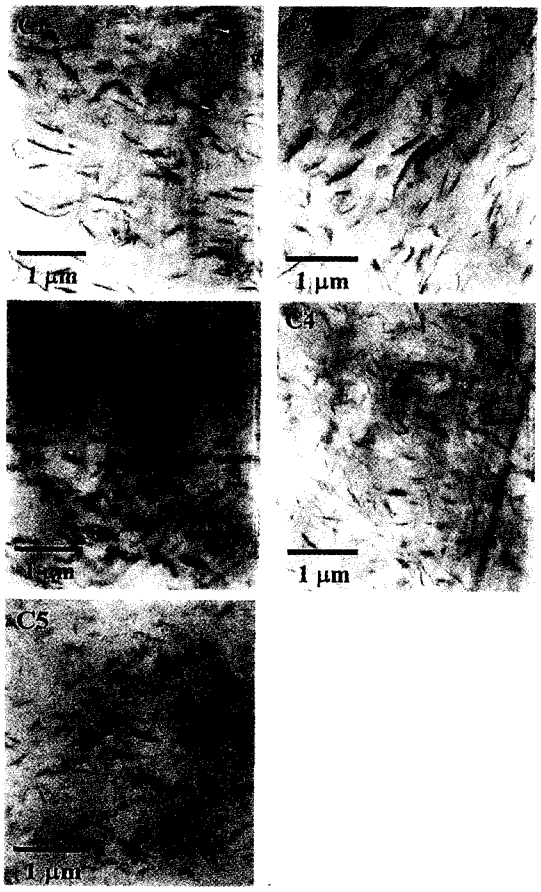

Figure 5. TEM micrographs of the clay/SAN hybrids with five different organophilic clays.

of clays using XRD method will be discussed in the later part. This might result from the fact that the dispersibility of silicate layers depends strongly upon the amount of intercalated SAN molecules into the inter-gallery of silicate layers. If the extent of transferred shear-force into a primary particle might be proportional to the amount of intercalated SAN molecules, the dispersibility of silicate layers becomes better as the change of basal spacing of the silicate layers, Δd in Figure 3(b), becomes larger. Thus the dispersibility of silicate layers becomes better as the amount of intercalated SAN molecules into silicate layers upon annealing the mixture of SAN and organophilic clay becomes larger.

The XRD peak intensities of the hybrids extruded with the twin screw extruder are shown in Figure 6(a), which shows that the peak intensity becomes smaller as the fraction of intercalant in the organophilic clay becomes lower. The peak intensity can be used as a measuring parameter for the crystallinity of silicate layers in the hybrids. Figure 6(b) is the plot of full width at half-maximum, β, from the XRD peak of various hybrids. The full width at half-maximum increases, which means that the size of the crystallites of silicate layers in the hybrid decreases, as the fraction of intercalant in the organophilic clay used in preparing the hybrid decreases. The integrated intensity may be used as an exact form for the crystallinity considering the broad XRD peak as following :

$$\text{crystallinity} \propto \int s^2 I(s) ds \qquad (2)$$

where s ($=2\sin\theta/\lambda$) is a scattering vector. If we neglect the effect of peak position on the calculated crystallinity of intercalated silicate layers, the crystallinity is assumed to be proportional to the area of (001) plane peak. Thus $\beta H/2$ may be used as a measuring parameter for the crystallinity of intercalated peak. Figure 6(c) is a plot of $\beta H/2$ for various hybrids. The plot shows that the crystallinity of intercalated silicate layers, $\beta H/2$, decreases as the fraction of intercalant in the organophilic clay becomes lower. This is consistent with the results found in TEM observation.

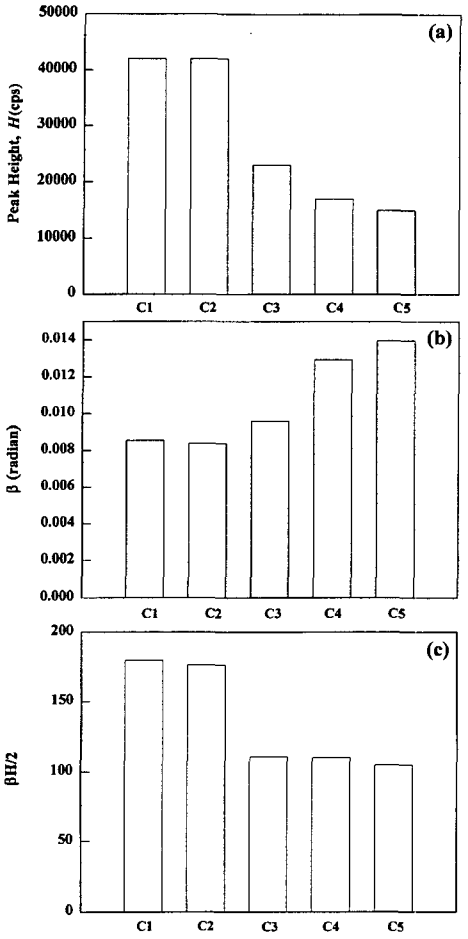

Figure 6. (a) Plot of the maximum peak intensity, H of silicate layers; (b) Plot of the full width at half maximum, β; (c) Plot of crystallinity of intercalated silicate layers in the various hybrids prepared using the twin screw extruder.

Mechanical Properties of Hybrids. Flexural properties of the composites were measured to examine the size effect of fillers on the reinforcement. The flexural moduli of the hybrids are plotted in Figure 7. Considering that the measured flexural modulus of pure SAN is 3.23 GPa, the flexural moduli of hybrids are larger than that of the pure SAN, but showing some different extent of reinforcement with the kind of the organophilic clays. The effect of stiffness reinforcement with the addition of clay can be found in any kind of hybrid, but it can be said that the effect of stiffness reinforcement of clay becomes greater as the dispersibility of silicate layers in the hybrids becomes

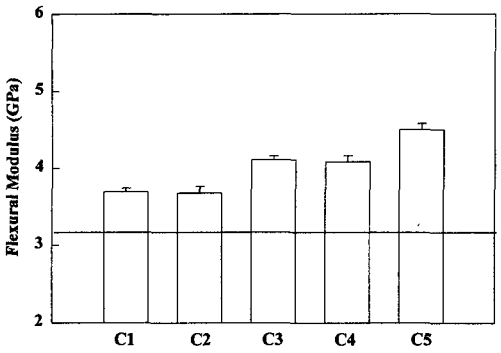

Figure 7. Flexural moduli for the clay/SAN hybrids with five different organophilic clays. The horizontal line represents the flexural modulus of the neat SAN copolymer.

better. As discussed in the earlier report,[21] the modulus of a hybrid depends strongly on the aspect ratio of dispersed filler in the hybrid. Therefore the aspect ratio of a dispersed nano-scale building block of clays in the hybrid increases as the dispersibility of silicate layers increases, assuming the same quantity of loaded inorganics.

Conclusions

Clay/SAN hybrids have been prepared by simple melt-mixing of two components, SAN and five different organophilic clays with a twin screw extruder. The dispersibility of 10-Å-thick silicate layers of clays in the hybrid was investigated by using X-ray diffraction method and transmission electron microscopy. It was found that high fraction of intercalant in organophilic clay leads to immiscibile phases in the mixture, resulting in poor intercalation of SAN, and thus worse dispersibility of silicate layers at 180°C. Even though any other evidence for truly exfoliated nanocomposite could not be found in this study, the nano-scale building block in the hybrids becomes smaller, showing better dispersibility of clay as the fraction of intercalant in the organophilic clay becomes low. This might be associated with the fact that the dispersibility of silicate layers depends strongly on the change of basal spacing of the silicate layers upon the intercalation of SAN molecules into the intergallery of silicate layers. Also, the flexural modulus of hybrids increases as the dispersibility of silicate layers in the hybrid increases.

Acknowledgements. This work was supported by the KIST-2000 project. The authors, also, would like to thank the Southern Clay Products Inc. for providing the organophilic clays.

References

(1) M. S. Wang and T. J. Pinavaia, *Chem. Mater.*, **6**, 468 (1994).
(2) P. B. Massersmith and E. P. Giannelis, *Chem. Mater.*, **6**,1719 (1994).
(3) T. Lan, P. D. Kaviratana, and T. J. Pinavaia,*Chem. Mater.*, **7**, 2144 (1995).
(4) S. D. Burnside and E. P. Gianellis,*Chem. Mater.*, **7**, 1597 (1995).
(5) R. A. Vaia, K. D. Jandt, E. J. Kramer, and E. P. Giannelis, *Macromolecules,* **28**, 8080 (1995).
(6) G. Jimenez, N. Ogata, H. Kawai, and T. Ogihara, *J. Appl. Polym. Sci.*, **64**, 2211 (1997).
(7) M. Kato, A. Usuki, and A. Okada, *J. Appl. Polym. Sci.*, **66**, 1781 (1997).
(8) M. Kawasumi, N. Hasegawa, M. Kato, A. Usuki, and A. Okada, *Macromolecules,* **30**, 333 (1997).
(9) N. Ogata, S. Kawakage, and T. Oghihara,*J. Appl. Polym. Sci.*, **66**, 573 (1997).
(10) N. Hasegawa, M. N. Kawasumi, M. Kato, A. Usuki, and A. Okada, *J. Appl. Polym. Sci.*, **67**, 87 (1998).
(11) D. Smock, *Modern Plastics,* **28**, No. 2, 28 (1998).
(12) E. Hackett, E. Manias, and E. P. Gianellis,*J. Chem. Phys.*, **108**, 7410 (1998).
(13) J. A. Grande, *Modern Plastics,* **29**, No. 1, 35 (1999).
(14) R. A. Vaia, H. Ishii, and E. P. Gianellis, *Chem. Mater.*, **5**, 1694 (1993).
(15) A. Akelah and A. Moet, *J. Mater. Sci.*, **31**, 3589 (1996).
(16) N. Hasegawa, H. Okamota, M. Kawasumi, and A. Usuki, *Proceedings of the ACS Division of Polymer Materials: Science and Engineering,* **80**, 353 (1999).
(17) G. Lagaly, *Clay Minerals,* **16**, 1 (1981).
(18) T. Lan, P. D. Kaviratna, and T. J. Pinnavaia, *J. Phys. Chem. Solids,* **57**, 1005 (1996).
(19) B. Török, M. Bartók, and I. Dékány,*Colloid Polym. Sci.*, **227**, 340 (1999).
(20) U. W. Gedde Ed., *Polymer Physics,* Chapman & Hall, London, 1995, pp 147.
(21) M. B. Ko, S. Lim, J. Kim, C. R. Choe, M. S. Lee and M. G. Ha, *Korea Polym. J.* **7**, No. 5, 310 (1999).